

A Family of Au–Tl Loosely Bound Butterfly Clusters

Eduardo J. Fernández,* José M. López-de-Luzuriaga, M. Elena Olmos, and Javier Pérez

Departamento de Química, Universidad de La Rioja, Grupo de Síntesis Química de La Rioja, UA-CSIC, Madre de Dios 51, E-26004 Logroño, Spain

Antonio Laguna*

Departamento de Química Inorgánica-ICMA, Universidad de Zaragoza-CSIC, E-50009 Zaragoza, Spain

M. Cristina Lagunas

School of Chemistry, The Queen's University of Belfast, Belfast BT9 5AG, U.K.

Received January 14, 2005

By treatment of the polymeric species $[\text{AuTl}(\text{C}_6\text{Cl}_5)_2]_n$ with ketones or with acetylacetone and 4,4'-bipyridine, the new tetranuclear complexes $[\text{Au}_2\text{Tl}_2(\text{C}_6\text{Cl}_5)_4]\cdot\text{L}$ ($\text{L} = \text{PhMeC}=\text{O}$, acacH) or $[\text{Au}_2\text{Tl}_2(\text{C}_6\text{Cl}_5)_4(\text{bipy})]\cdot(\text{acacH})$ have been prepared. Their crystal structures have been determined by X-ray diffraction methods and they all present a central Au_2Tl_2 core formed via one $\text{Tl}\cdots\text{Tl}$ and four $\text{Au}\cdots\text{Tl}$ unsupported interactions resulting in a loosely bound butterfly cluster. These complexes are strongly luminescent in both the solid state and solution showing an optical behavior in agreement with the maintenance of the $\text{Tl}\cdots\text{Tl}$ contact even in solution.

Introduction

Recent research has focused on understanding *metallophilic* attractions prompted by the unpredictable and large variety of structural dispositions and networks observed as a result of the attraction between certain closed-shell metals. The most common are probably those found between gold atoms. Thus, *aurophilic* attractions have been observed in a variety of mono- and poly-nuclear gold(I) species and have been described in recent experimental and theoretical reviews.¹ Short metal–metal contacts in the solid state are of great interest because of their influence on the molecular structure and physical properties of the materials in which they are present, such as luminescence. An usual effect observed in these complexes is an enhancement of the emissions and, consequently, brightly emissive compounds are obtained. Moreover, the spectroscopic properties of such species can be useful for the development of, for example, volatile organic vapors (VOCs) sensors² or light emitting devices (LEDs).³

The most recent studies of metallophilicity have focused on gold(I)-containing heterometallic systems, and the synthesis of complexes containing $\text{Au}^{\text{I}}\text{–Pd}^{\text{II}}$, $\text{Au}^{\text{I}}\text{–Au}^{\text{III}}$ ($d^{10}\text{–}d^8$), $\text{Au}^{\text{I}}\text{–Ag}^{\text{I}}$, $\text{Au}^{\text{I}}\text{–Cu}^{\text{I}}$ ($d^{10}\text{–}d^{10}$), or $\text{Au}^{\text{I}}\text{–Tl}^{\text{I}}$ ($d^{10}\text{–}s^2$) interactions have made their theoretical study possible.^{4–6}

For the synthesis of this type of complexes, our group has employed a synthetic strategy based on the reaction between basic gold(I) complexes of the type $[\text{Au}(\text{C}_6\text{X}_5)_2]^-$ ($\text{X} = \text{F}, \text{Cl}, \dots$) and Lewis acids such as Ag^+ or Tl^+ .^{2c,6,7} Perhaps, the

- (2) (a) Buss, C. E.; Mann, K. R. *J. Am. Chem. Soc.* **2002**, *124*, 1031. (b) Mansour, M. A.; Connick, W. B.; Lachicotte, R. J.; Gysling, H. J.; Eisenberg, R. *J. Am. Chem. Soc.* **1998**, *120*, 1329. (c) Fernández, E. J.; López-de-Luzuriaga, J. M.; Monge, M.; Olmos, M. E.; Pérez, J.; Laguna, A.; Mohamed, A. A.; Fackler, J. P., Jr. *J. Am. Chem. Soc.* **2003**, *125*, 2022. (d) Fernández, E. J.; López-de-Luzuriaga, J. M.; Monge, M.; Montiel, M.; Olmos, M. E.; Pérez, J.; Laguna, A.; Mendizábal, F.; Mohamed, A. A.; Fackler, J. P., Jr. *Inorg. Chem.* **2004**, *43*, 3573.
- (3) Lamansky, S.; Djurovich, P.; Murphy, D.; Abdel-Razzaq, F.; Lee, H.; Adachi, C.; Burrows, P. E.; Forrest, S. R.; Thompson, M. E. *J. Am. Chem. Soc.* **2001**, *123*, 4304.
- (4) (a) Crespo, O.; Laguna, A.; Fernández, E. J.; López-de-Luzuriaga, J. M.; Jones, P. G.; Teichert, M.; Monge, M.; Pyykkö, P.; Runeberg, N.; Schütz, M.; Werner, H.-J. *Inorg. Chem.* **2000**, *39*, 4786. (b) Canales, S.; Crespo, O.; Gimeno, M. C.; Jones, P. G.; Laguna, A.; Mendizábal, F. *Organometallics* **2001**, *20*, 4812. (c) Mendizábal, F.; Pyykkö, P. *Phys. Chem. Chem. Phys.* **2004**, *6*, 900. (d) Mendizábal, F.; Zapata-Torres, G.; Olea-Azar, C. *Chem. Phys. Lett.* **2003**, *382*, 92.

* To whom correspondence should be addressed. E-mail: eduardo.fernandez@dq.unirioja.es (E.J.F.); alaguna@unizar.es (A.L.).

(1) Pyykkö, P. *Chem. Rev.* **1997**, *97*, 597.

most interesting of these reactions is that of $\text{NBu}_4[\text{Au}(\text{C}_6\text{Cl}_5)_2]$ with TIPF_6 , which is highly dependent on reaction conditions such as solvent, presence of ligands, etc. It leads to a wide variety of heteronuclear complexes classified as noncluster species, which range from discrete molecules^{7c,8} to larger supramolecular assemblies such as extended chains^{2c,2d,6,9} or two-^{7b,9,10} or three-¹⁰ dimensional networks built only with what are generally considered to be “weak” metal–metal interactions. Among them, the most striking one is the loosely bound butterfly cluster $[\text{Au}_2\text{Tl}_2(\text{C}_6\text{Cl}_5)_4] \cdot (\text{Me}_2\text{C}=\text{O})$,^{7c} which is obtained from the reaction of the aforementioned precursors in acetone, and it displays a $\text{Tl} \cdots \text{Tl}$ interaction, which is even claimed to remain in solution, that seems to be responsible for its interesting optical properties.

In contrast, the polymeric species $[\text{AuTl}(\text{C}_6\text{Cl}_5)_2]_n$, which displays a perfectly linear polymetallic chain,^{2c} is synthesized using THF as solvent and has proven to be extremely reactive toward a variety of ligands both in solution^{2d,9,10} and in the solid state,^{2d} yielding a polymeric species in which the extended polymetallic chain formed by alternating gold and thallium interacting centers is maintained. Thus, for example, its treatment with 4,4'-bipyridine (bipy) in different molar ratios, solvents, or both gives rise to a wide variety of polymeric materials, which contain different amounts of bipy and display two- or three-dimensional networks in the solid state.

Taking these results into account, we tried to prepare complexes that retained the tetranuclear core $[\text{Au}_2\text{Tl}_2(\text{C}_6\text{Cl}_5)_4]$ by reacting the polymeric material $[\text{AuTl}(\text{C}_6\text{Cl}_5)_2]_n$ with ketones, even in the presence of more donor and versatile ligands, such as 4,4'-bipyridine. We were also interested in the study of their optical properties and the stability of the $\text{Tl} \cdots \text{Tl}$ interaction in solution.

This paper describes the synthesis, structural analysis, and photophysical studies of a series of gold/thallium tetranuclear compounds obtained by treating $[\text{AuTl}(\text{C}_6\text{Cl}_5)_2]_n$ with acetone, acetophenone, acetylacetone, or acetylacetone and 4,4'-bipyridine. They all have a tetranuclear core formed via one $\text{Tl} \cdots \text{Tl}$ and four $\text{Au} \cdots \text{Tl}$ interactions, resulting in loosely

bound butterfly clusters with very interesting optical properties.

Experimental Section

Instrumentation. Infrared spectra were recorded in the range of 4000–200 cm^{-1} on a Perkin-Elmer FT-IR Spectrum 1000 spectrophotometer using Nujol mulls between polyethylene sheets. Conductivity was measured in ca. 5×10^{-4} M acetone solutions with a Jenway 4010 conductimeter. C, H, and N analyses were carried out with a Perkin-Elmer 240C microanalyzer. Mass spectra were recorded on a HP59987 A ELECTROSPRAY. ¹H NMR spectra were recorded on a Bruker ARX 300 in THF-*d*₈ solutions. Chemical shifts are quoted relative to SiMe_4 (¹H, external). UV–vis absorption spectra were obtained on a HP-8453 UV–vis recording spectrophotometer in acetonitrile solutions (1×10^{-5} M). Excitation and emission spectra were recorded on a Jobin-Yvon Horiba Fluorolog 3–22 Tau-3 spectrofluorimeter. Fluorescence lifetime was also recorded with a Jobin-Yvon Horiba Fluorolog 3–22 Tau-3 spectrofluorimeter operating in the phase-modulation mode. Phase shift and modulation were recorded over the frequency range of 0.2–50 MHz, and the data were fitted using the Jobin-Yvon software package. Powder X-ray diffraction data were collected on a PANalytical X'Pert Pro diffractometer with $\text{Cu K}\alpha$ radiation. Gold L_{III} EXAFS spectra were recorded at the Daresbury SRS on station 16.5 in transmission (solid) or fluorescence (solution) mode. A 13-element solid-state Canberra fluorescence detector was used for the latter. For measurements in the solid state, compound **1** was ground with polyvinylpyrrolidone or boron nitride and pressed into a pellet of 1–2 mm thickness. Acetone solutions (ca. 10^{-2} M) were placed between polyethylene windows separated ca. 5–10 mm. The scans were averaged using EXCALIB, which was also used to convert the raw data into energy versus absorption data. EXBROOK was used to remove the background, and the analysis of the EXAFS data was performed using EXCURV98 on the raw data.

General. Acetylacetone, 4,4'-bipyridine, and acetophenone are commercially available; they were purchased from ACROS and used as received. The precursor complex $[\text{AuTl}(\text{C}_6\text{Cl}_5)_2]_n$ was obtained according to the literature procedure.^{2c}

Preparation of $[\text{Au}_2\text{Tl}_2(\text{C}_6\text{Cl}_5)_4] \cdot (\text{Me}_2\text{CO})$ (1**) and $[\text{Au}_2\text{Tl}_2(\text{C}_6\text{Cl}_5)_4] \cdot (\text{PhMeCO})$ (**2**).** A solution of 0.09 g (0.1 mmol) of $[\text{AuTl}(\text{C}_6\text{Cl}_5)_2]_n$ in 10 mL of acetone (**1**) or acetophenone (**2**) was stirred for 30 min. The slow evaporation of the solvent produced a pale yellow solid in both cases. Yield: 100%. Complex **2**. Elemental analysis calcd (%) for $\text{C}_{32}\text{H}_8\text{Au}_2\text{Cl}_{20}\text{OTl}_2$: C, 19.85; H, 0.4. Found: C, 20.0; H, 0.4. IR: $\nu(\text{C}_6\text{Cl}_5)$ at 839 and 615 cm^{-1} ; $\nu(\text{C}=\text{O})$ at 1660 and 1650 cm^{-1} . ¹H NMR (RT, THF-*d*₈): δ 7.96–7.41 (m, 5H, Ph), 2.53 (s, 3H, CH₃). Mass spectra: ES+ m/z = 204 (100%), $[\text{Tl}]^+$; ES– m/z = 695 (100%), $[\text{Au}(\text{C}_6\text{Cl}_5)_2]^-$.

Preparation of $[\text{Au}_2\text{Tl}_2(\text{C}_6\text{Cl}_5)_4] \cdot (\text{acacH})$ (3**).** Fifty-one microliters (0.5 mmol) of acacH was added to a suspension of 0.09 g (0.1 mmol) of $[\text{AuTl}(\text{C}_6\text{Cl}_5)_2]_n$ in toluene (15 mL). The mixture was stirred for 30 min, and the solvent was concentrated in vacuo to 5 mL. The addition of *n*-hexane led to the precipitation of **3** as a pale yellow solid. Yield: 72%. Elemental analysis calcd (%) for $\text{C}_{29}\text{H}_8\text{Au}_2\text{Cl}_{20}\text{O}_2\text{Tl}_2$: C, 18.5; H, 0.5. Found: C, 18.35; H, 0.45. IR: $\nu(\text{C}_6\text{Cl}_5)$ at 840 and 615 cm^{-1} ; $\nu(\text{C}=\text{O})$ at 1732 and 1608 cm^{-1} . ¹H NMR (RT, THF-*d*₈): δ 3.56 (s, 2H, CH₂), 2.19 (s, 6H, CH₃) for the keto form; 5.55 (s, 1H, CH), 1.99 ppm (s, 6H, CH₃) for the enol form. Mass spectra: ES+ m/z = 204 (100%), $[\text{Tl}]^+$; ES– m/z = 695 (100%), $[\text{Au}(\text{C}_6\text{Cl}_5)_2]^-$.

Preparation of $[\text{Au}_2\text{Tl}_2(\text{C}_6\text{Cl}_5)_4(\text{bipy})] \cdot (\text{acacH})$ (4**).** 4,4'-Bipyridine (0.016 g, 0.1 mmol) was added to a suspension of 0.19 g

- (5) (a) Pyykkö, P.; Runeberg, N.; Mendizábal, F. *Chem. Eur. J.* **1997**, *3*, 1451. (b) Fernández, E. J.; López-de-Luzuriaga, J. M.; Monge, M.; Rodríguez, M. A.; Crespo, O.; Gimeno, M. C.; Laguna, A.; Jones, P. G. *Chem. Eur. J.* **2000**, *6*, 636. (c) Fernández, E. J.; López-de-Luzuriaga, J. M.; Crespo, O.; Laguna, A.; Jones, P. G.; Monge, M.; Pyykkö, P.; Runeberg, N. *Eur. J. Inorg. Chem.* **2002**, 750.
- (6) Fernández, E. J.; Laguna, A.; López-de-Luzuriaga, J. M.; Mendizábal, F.; Monge, M.; Olmos, M. E.; Pérez, J. *Chem. Eur. J.* **2003**, *9*, 456.
- (7) (a) Crespo, O.; Fernández, E. J.; Jones, P. G.; Laguna, A.; López-de-Luzuriaga, J. M.; Mendía, A.; Monge, M.; Olmos, M. E. *Chem. Commun.* **1998**, 2233. (b) Fernández, E. J.; Jones, P. G.; Laguna, A.; López-de-Luzuriaga, J. M.; Monge, M.; Olmos, M. E.; Pérez, J. *Inorg. Chem.* **2002**, *41*, 1056. (c) Fernández, E. J.; Laguna, A.; López-de-Luzuriaga, J. M.; Monge, M.; Olmos, M. E.; Pérez, J. *J. Am. Chem. Soc.* **2002**, *124*, 5942.
- (8) Fernández, E. J.; Laguna, A.; López-de-Luzuriaga, J. M.; Olmos, M. E.; Pérez, J. *Chem. Commun.* **2003**, 1760.
- (9) Fernández, E. J.; Laguna, A.; López-de-Luzuriaga, J. M.; Monge, M.; Montiel, M.; Olmos, M. E.; Pérez, J. *Organometallics* **2004**, *23*, 774–782.
- (10) Fernández, E. J.; Laguna, A.; López-de-Luzuriaga, J. M.; Olmos, M. E.; Pérez, J. *Dalton Trans.* **2004**, 1801.

Table 1. Details of Data Collection and Structure Refinement for Complexes **2**, **3**, and **4**

	2	3	4
chemical formula	C ₃₂ H ₈ Au ₂ Cl ₂₀ OTl ₂	C ₂₉ H ₈ Au ₂ Cl ₂₀ O ₂ Tl ₂	C ₄₆ H ₂₄ Au ₂ Cl ₂₀ N ₂ O ₂ Tl ₂
cryst color	pale yellow	yellow	pink
cryst size (mm)	0.25 × 0.1 × 0.1	0.12 × 0.1 × 0.1	0.30 × 0.25 × 0.25
cryst syst	triclinic	triclinic	triclinic
space group	<i>P</i> $\bar{1}$	<i>P</i> $\bar{1}$	<i>P</i> $\bar{1}$
<i>a</i> (Å)	10.3500(1)	10.2987(1)	11.4069(1)
<i>b</i> (Å)	14.1622(2)	14.1347(2)	14.3783(2)
<i>c</i> (Å)	14.7297(2)	14.6246(2)	17.8738(2)
α (deg)	88.1049(6)	86.7517(8)	97.3468(7)
β (deg)	88.2305(6)	87.7151(8)	103.2596(6)
γ (deg)	85.0893(7)	85.4059(6)	96.4217(6)
<i>U</i> (Å ³)	2149.11(5)	2115.25(5)	2148.35
<i>Z</i>	2	2	2
<i>D</i> _c (g cm ⁻³)	2.967	2.983	2.549
<i>F</i> (000)	1736	1716	1980
<i>T</i> (K)	223(2)	173(2)	173(2)
2 θ _{max} (deg)	56	56	56
μ (Mo K α) (mm ⁻¹)	15.557	15.806	11.960
no. of reflns measured	34919	37190	40565
no. of unique reflns	10215	8884	13323
<i>R</i> _{int}	0.041	0.0490	0.0460
<i>R</i> ^a (<i>I</i> > 2 σ (<i>I</i>))	0.0378	0.0309	0.0309
<i>R</i> _w ^b (<i>F</i> ² , all reflns)	0.1146	0.0556	0.0733
no. of parameters	515	499	671
no. of restraints	156	141	209
<i>S</i> ^c	1.059	1.014	1.034
max. residual electron density (e Å ⁻³)	3.102	3.783	1.554

^a $R(F) = \sum ||F_o| - |F_c|| / \sum |F_o|$. ^b $R_w(F^2) = [\sum \{w(F_o^2 - F_c^2)^2\} / \sum \{w(F_o^2)^2\}]^{0.5}$; $w^{-1} = \sigma^2(F_o^2) + (aP)^2 + bP$, where $P = [F_o^2 + 2F_c^2]/3$ and *a* and *b* are constants adjusted by the program. ^c $S = [\sum \{w(F_o^2 - F_c^2)^2\} / (n - p)]^{0.5}$, where *n* is the number of data and *p* the number of parameters.

(0.1 mmol) of **3** in toluene (15 mL). The mixture was stirred for 30 min, and the solvent was concentrated in vacuo to 5 mL. The addition of *n*-hexane led to the precipitation of **4** as a salmon solid. Yield: 75%. Elemental analysis calcd (%) for C₃₉H₁₆Au₂Cl₂₀O₂-Tl₂N₂: C, 24.1; H, 0.9; N, 1.35. Found: C, 24.5; H, 1.0; N, 1.5. IR: ν (C₆Cl₅) at 839 and 619 cm⁻¹; ν (C=O) at 1735 and 1652 cm⁻¹; ν (C=N) at 1795 and 1566 cm⁻¹. ¹H NMR (RT, THF-*d*₈): δ 3.56 (s, 2H, CH₂), 2.19 (s, 6H, CH₃) for the keto form; 5.55 (s, 1H, CH), 1.99 (s, 6H, CH₃) for the enol form; 8.66 (m, 4H, CH), 7.66 (m, 4H, CH) for the bipyridine ligand. Mass spectra: ES⁺ *m/z* = 204 (100%), [Tl]⁺; ES⁻ *m/z* = 695 (100%), [Au(C₆Cl₅)₂]⁻.

Crystallography. Crystals were mounted in inert oil on glass fibers and transferred to the cold gas stream of a Nonius Kappa CCD diffractometer equipped with an Oxford Instruments low-temperature attachment. Data were collected using monochromated Mo K α radiation ($\lambda = 0.71073$ Å) with scan type ω and ϕ . Numerical absorption corrections were made on the basis of multiple scans. The structures were solved by direct methods and refined on *F*² using the program SHELXL-97.¹¹ All non-hydrogen atoms were refined anisotropically. Hydrogen atoms were included using riding or rotating modes. All aromatic rings were restrained to improve their geometry. Further details of the data collection and refinement are given in Table 1. Selected bond lengths and angles are presented in Tables 2–5, and the crystal structures of complexes **2**–**4** appear in Figures 1–4.

Result and Discussion

Synthesis and Characterization. We have recently described the synthesis of the tetranuclear complex [Au₂-Tl₂(C₆Cl₅)₄](Me₂C=O) (**1**) by treating NBu₄[Au(C₆Cl₅)₂] with TIPF₆ in acetone.^{7c} The same product can also be obtained when the polymeric [AuTl(C₆Cl₅)₂]_{*n*} is dissolved

Table 2. Selected Bond Lengths (Å) and Angles (deg) for Complex **2**^a

Au(1)–Tl(2)	3.0167(4)	Au(1)–Tl(1)	3.2313(4)
Au(2)–Tl(1)	3.1071(4)	Au(2)–Tl(2)	3.1102(3)
Au(1)–C(1)	2.052(6)	Au(1)–C(11)	2.062(7)
Au(2)–C(21)	2.062(6)	Au(2)–C(31)	2.065(7)
Tl(1)–O	2.713(5)	Tl(2)–O	3.086(6)
Tl(1)–Tl(2)	3.7110(4)		
C(1)–Au(1)–C(11)	178.0(2)	Tl(2)–Au(1)–Tl(1)	72.78(1)
C(21)–Au(2)–C(31)	173.7(2)	Tl(1)–Au(2)–Tl(2)	73.29(1)
Au(2)–Tl(1)–Au(1)	100.07(1)	Au(1)–Tl(2)–Au(2)	104.92(1)
Au(1)–Tl(2)–Tl(1)	56.28(1)		

^a Symmetry transformations used to generate equivalent atoms: #1 $-x + 1, -y + 1, -z + 1$.

Table 3. Selected Bond Lengths (Å) and Angles (deg) for Complex **3**^a

Au(1)–Tl(2)	3.0852(4)	Au(1)–Tl(1)	3.1326(4)
Au(2)–Tl(2)	3.0990(4)	Au(2)–Tl(1)	3.1237(4)
Au(1)–C(11)	2.056(6)	Au(1)–C(1)	2.058(6)
Au(2)–C(31)	2.050(6)	Au(2)–C(21)	2.066(6)
Tl(1)–O(1)	2.826(5)	Tl(1)–Tl(2)	3.7152(4)
O(1)–C(41)	1.277(8)	O(2)–C(43)	1.314(9)
C(11)–Au(1)–C(1)	178.0(2)	Tl(2)–Au(1)–Tl(1)	73.38(1)
C(31)–Au(2)–C(21)	174.6(2)	Tl(2)–Au(2)–Tl(1)	73.31(1)
Au(2)–Tl(1)–Au(1)	101.26(1)	Au(1)–Tl(2)–Au(2)	102.90(1)
C(43)–C(42)–C(41)	122.8(8)		

^a Symmetry transformations used to generate equivalent atoms: #1 $-x, -y + 1, -z + 1$.

in acetone, and the solution is evaporated in vacuo. Similarly, when acetophenone is employed instead of acetone, [Au₂-Tl₂(C₆Cl₅)₄](PhMeC=O) (**2**) is isolated after evaporation of the solvent. Both complexes are obtained as pale yellow solids.

In contrast, when the same procedure is followed using acetylacetone as the solvent, the polymeric species {Tl-(acacH)₂[Au(C₆Cl₅)₂]_{*n*}, with two molecules of acetylacetone

(11) Sheldrick, G. M. *SHELXL-97*, A program for crystal structure refinement; University of Göttingen: Göttingen, Germany, 1997.

Table 4. Selected Bond Lengths (Å) and Angles (deg) for Complex 4^a

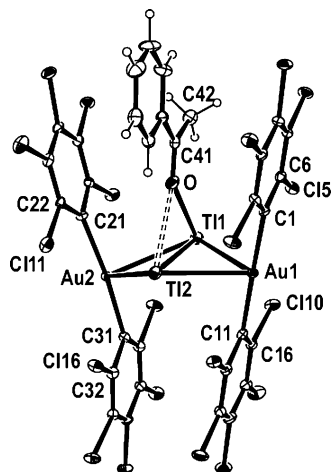
Au(1)–Tl(2)	3.2133(3)	Au(1)–Tl(1)	3.2414(3)
Au(2)–Tl(2)	3.0314(3)	Au(2)–Tl(1)	3.2349(3)
Au(1)–C(11)	2.052(5)	Au(1)–C(1)	2.056(5)
Au(2)–C(31)	2.056(5)	Au(2)–C(21)	2.056(5)
Tl(1)–N(51)	2.874(5)	Tl(1)–Tl(2)	3.6263(3)
Tl(1)–O(2)	2.959(4)	Tl(1)–O(1)	2.904(4)
Tl(2)–O(1)	2.707(4)	O(1)–C(41)	1.238(7)
O(2)–C(43)	1.324(7)		
C(11)–Au(1)–C(1)	174.54(18)	Tl(2)–Au(1)–Tl(1)	68.36(1)
C(31)–Au(2)–C(21)	177.75(18)	Tl(2)–Au(2)–Tl(1)	70.63(1)
Au(2)–Tl(1)–Au(1)	99.60(1)	N(51)–Tl(1)–Tl(2)	164.85(10)
Au(2)–Tl(2)–Au(1)	104.73(1)	C(43)–C(42)–C(41)	127.6(5)

^a Symmetry transformations used to generate equivalent atoms: #1 $-x + 2, -y, -z + 1$.

Table 5. Hydrogen Bond Lengths (Å) and Angles (deg) for Complexes 3 and 4^a

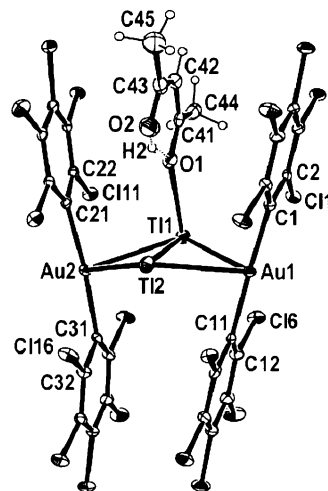
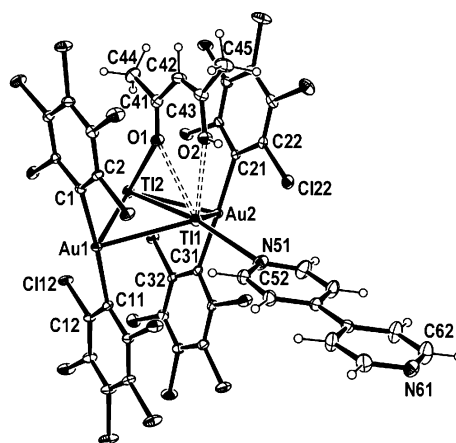
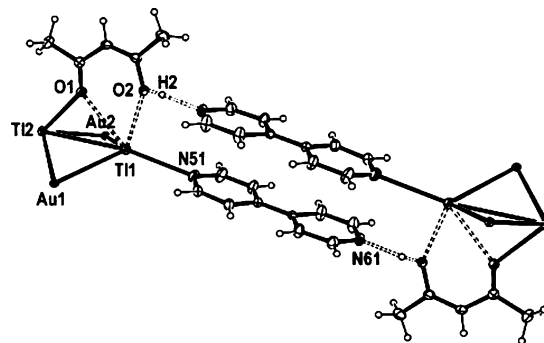
	D–H···A	d(D–H)	d(H···A)	d(D···A)	∠(DHA)
3	O(2)–H(2)···O(1)	0.82	1.83	2.553(7)	146.7
4	O(2)–H(2)···N(61)#1	0.84	1.81	2.641(6)	171.6

^a Symmetry transformations used to generate equivalent atoms: #1 $-x + 3, -y, -z + 2$.

**Figure 1.** Molecular structure of complex 2 (30% probability level) with the labeling scheme of the atom positions.

coordinated to each thallium center,^{2d} is obtained. However, the reaction of $[\text{AuTl}(\text{C}_6\text{Cl}_5)_2]_n$ with acetylacetonate (2:1) in toluene produces the expected result, $[\text{Au}_2\text{Tl}_2(\text{C}_6\text{Cl}_5)_4] \cdot (\text{acacH})$ (**3**), which is isolated as a pale yellow solid. Finally, the complex $[\text{Au}_2\text{Tl}_2(\text{C}_6\text{Cl}_5)_4(\text{bipy})] \cdot (\text{acacH})$ (**4**) is obtained as a salmon pink solid from the reaction of **3** with 1 equiv of 4,4'-bipyridine (bipy) in toluene.

Complexes **2–4** are soluble in acetone and tetrahydrofuran and insoluble in diethyl ether and *n*-hexane. Solutions of these complexes are stable in air and moisture for days or weeks. Their elemental analyses and physical and spectroscopic properties are in accordance with the proposed stoichiometries. Thus, their ¹H NMR spectra in THF-*d*₈ show the signals corresponding to the ketones at the same chemical shift as for the free ligands, which could indicate a dissociative equilibrium of the ligands in the donor THF solutions, where an exchange process could occur and a variety of species in equilibrium could exist. Moreover, in the case of complexes **3** and **4**, the acetylacetonate signals in their ¹H NMR spectra show the presence of a keto–enol equilibrium

**Figure 2.** Molecular structure of complex 3 (30% probability level) with the labeling scheme of the atom positions.**Figure 3.** Molecular structure of complex 4 (30% probability level) with the labeling scheme of the atom positions.**Figure 4.** Dimerization of **4** through intermolecular hydrogen bonds. C₆–Cl₅ groups are omitted for clarity.

as observed in the free ligand. Last, the ¹H NMR spectrum of **4** displays two multiplets at 8.66 and 7.66 ppm, corresponding to the protons of the bidentate ligand bipy and whose integration reveal the presence of equimolar amounts of this ligand and acacH in the product. This result could be in accordance with the substitution of the ligands by THF molecules, whose affinity for the thallium atoms is higher.¹⁰

Their IR spectra show the absorptions from the C₆Cl₅ groups bonded to gold(I) at 839 (s) and 615 cm⁻¹ (m), as well as strong absorptions assigned to the stretching $\nu(\text{C}=\text{C})$

O) vibration in the ketone molecules at 1660 and 1650 (**2**), 1732 and 1608 (**3**), and 1735 and 1652 cm^{-1} (**4**). These bands are shifted if compared to those observed in the free ketones: 1686 and 1646 cm^{-1} for acetophenone and 1729 and 1622 cm^{-1} for acetylacetone.¹² In addition, complex **4** shows two absorptions at 1595 and 1566 cm^{-1} from the stretching $\nu(\text{N}=\text{C})$ vibration in the 4,4'-bipyridine molecules, which are also shifted if compared to the IR of the free ligand (1587 and 1532 cm^{-1}).¹² Solution IR measurements show bands consistent with the presence of free ligands in the solution.

The powder X-ray diffraction (XRD) pattern of **1** is in good agreement with that simulated from the single-crystal diffraction data (see Supporting Information) confirming that the latter accurately represents the structure of the bulk solid. Gold L_{III} EXAFS studies at room temperature were performed on complex **1** both in the solid state and in a concentrated solution of acetone (10^{-2} M). The spectra were recorded out to $k = 13 \text{ \AA}^{-1}$, but the signal-to-noise ratio obtained was very poor at $k > 7 \text{ \AA}^{-1}$. The use of polyvinylpyrrolidone or boron nitride as substrate in the preparation of solid samples did not significantly affect the quality of the data. Attempts to extract structural information using the EXAFS data obtained were unsuccessful. However, the similarity of the EXAFS spectra for the samples in the solid state and in solution seems to indicate that the structures of **1** in the solid state and when dissolved in acetone 10^{-2} M are similar, in agreement with the luminescence data.

Finally, equivalent conductivity measurements of these complexes in acetonitrile over the range 10^{-4} – 10^{-3} mol/L present values of 1100 ($\Lambda_0 = 127.0$, $R^2 = 0.992$) for complex **1**, 1118 ($\Lambda_0 = 127.7$, $R^2 = 0.998$) for **2** and 1284 ($\Lambda_0 = 129.9$, $R^2 = 0.990$) for **4** for A in Onsager's equation ($\Lambda_e = \Lambda_0 - A_c^{1/2}$). Unfortunately, complex **3** shows very low solubility in acetonitrile, which prevented the measurement of its equivalent conductivity. These values are in the range corresponding to a 2:1 electrolyte,¹³ and their similarity could indicate that the complexes behave in the same way when their solutions are exposed to an electrical field. The interpretation of these measurements could suggest, in accordance with our previous proposal,^{7c} the existence of a thallium–thallium interaction in solution. This is probably stabilized by coordination of solvent molecules to the thallium atoms, in particular at low concentrations, where the dissociation of the $[\text{Au}(\text{C}_6\text{Cl}_5)_2]^-$ and $[\text{Tl}_2(\text{solvent})_x]^{2+}$ ions is more favored than in concentrated solutions. This could be the explanation for the apparent contradiction between the EXAFS and conductivity and NMR measurements. In addition, it is also possible that a variety of species are in equilibrium.

Crystal Structures. The crystal structures of complexes **2–4** (see Figures 1–4 and Tables 1–5) have been established by X-ray diffraction studies from single crystals

obtained by slow diffusion of *n*-hexane into solutions of the complexes in toluene (**2**, **3**, and **4**). They all show a central core in common with the crystal structure of complex **1**, as reported previously,^{7c} consisting of a tetranuclear unit with two thallium(I) and two gold(I) atoms held together through one $\text{Tl}\cdots\text{Tl}$ and four unsupported $\text{Au}\cdots\text{Tl}$ interactions resulting in a loosely bound butterfly cluster. The Au–Tl distances, within the 3.0167(4)–3.2414(3) \AA range, are similar to those in **1** (3.0331(6)–3.1887(6) \AA) and in most of the polymeric species with unsupported $\text{Au}\cdots\text{Tl}$ interactions.^{2c,2d,6,7,9,10} Regarding the $\text{Tl}\cdots\text{Tl}$ interaction, it is longer in **2** (3.7110(4) \AA) and **3** (3.7152(4) \AA) than in complex **4** (3.6263(3) \AA), the latter being similar to those in **1** (3.6027(6) \AA) and $[\text{Tl}_2\text{CNET}_2]_2$ ¹⁴ (3.60 and 3.62 \AA). Since **1** and **2** should be electronically very similar, the difference in their Tl–Tl distance could be the result of the greater bulk of the ketone in **2** if compared to that in **1**. Moreover, they are all longer than the intramolecular Tl–Tl distances found in $\text{Tl}[\text{C}(\text{SiMe}_3)_3]$ ¹⁵ (average 3.452 \AA) as well as the closest metal–metal distances in α -thallium¹⁶ (3.408 and 3.457 \AA), although they are shorter than the distances in $[\text{H}_3\text{CC}\{\text{CH}_2\text{N}(\text{Tl})\text{SiMe}_3\}_3]_2$ ¹⁷ (3.706(3)–3.807(4) \AA) or 1,3,5,7-tetraazaheptatrienylthallium(I)¹⁸ (3.759(1)–4.000(1) \AA).

The gold centers are almost linearly coordinated to two pentachlorophenyl groups with typical Au–C distances within the 2.050(6)–2.066(6) \AA range. On the other hand, the thallium atoms interact with the oxygen atoms of the ketone present in each complex, showing differences in the strength of these interactions. Thus, in complex **2**, Tl(1) binds the oxygen of the acetophenone molecule with a distance of 2.713(5) \AA , which is shorter than the distances found in $\{\text{trans,trans,trans-}[\text{PtTl}_2(\text{C}_6\text{F}_5)_2(\text{C}\equiv\text{C}^t\text{Bu})_2](\text{acetone})_2\}_n$ ¹⁹ (2.83(2) \AA) or $[\text{Au}(\text{C}_6\text{Cl}_5)_2]_2[\text{Tl}(\text{OPPh}_3)] [\text{Tl}(\text{OPPh}_3)(\text{acetone})]$ (2.828(7) \AA),^{7b} while Tl(2) shows only a weak interaction with the oxygen atom (Tl–O = 3.086(6) \AA). This distance is slightly longer than those in **1** (2.968(9) and 2.903(9) \AA), where both thallium centers display weak interactions with the oxygen atom of the acetone molecule.

In both crystal structures of **3** and **4**, one Tl^+ is bonded to the oxygen atom of acetylacetone in the keto form with Tl–O distances of 2.826(5) and 2.707(4) \AA , respectively. The distance in **3** compares well with those found in $\{\text{trans,trans,trans-}[\text{PtTl}_2(\text{C}_6\text{F}_5)_2(\text{C}\equiv\text{C}^t\text{Bu})_2](\text{acetone})_2\}_n$ ¹⁹ (2.83(2) \AA) and $[\text{Au}(\text{C}_6\text{Cl}_5)_2]_2[\text{Tl}(\text{OPPh}_3)][\text{Tl}(\text{OPPh}_3)(\text{acetone})]$ (2.828(7) \AA)⁶ and corresponds to a very weak bond, while the Tl–O bond distance in **4** is similar to the shorter one in **2**. In contrast, the second thallium center displays a different environment in both complexes. Thus, while in **3**, it only displays the previously mentioned $\text{Au}\cdots\text{Tl}$ interactions, in

(14) Pritzkow, H.; Jennische, P. *Acta Chem. Scand.* **1975**, A29, 60.

(15) Uhl, W.; Keimling, S. U.; Klinkhammer, K. W.; Schwarz, W. *Angew. Chem., Int. Ed. Engl.* **1997**, 36, 64.

(16) Pearson, W. B. *Handbook of Lattice Spacing and Structures of Metals*, Vol. 2; Pergamon Press: Oxford, U.K., 1967.

(17) Hellmann, K. W.; Gade, L. H.; Fleischer, R.; Kottke, T. *Chem. Eur. J.* **1997**, 3, 1801.

(18) Boesveld, W. M.; Hitchcock, P. B.; Lappert, M. F.; Nöth, H. *Angew. Chem., Int. Ed.* **2000**, 39, 222.

(19) Ara, I.; Berenguer, J. R.; Forniés, J.; Gómez, J.; Lalinde, E.; Merino, R. I. *Inorg. Chem.* **1997**, 36, 6461.

(12) (a) <http://www.aist.go.jp/RIODB/SDBS/menu-e.html> (b) Nakamoto, K. *Infrared and Raman Spectra of Inorganic and Coordination Compounds*; John Wiley and Sons: New York, 1986; pp 206 and 259.

(13) (a) Geary, W. *Coord. Chem. Rev.* **1971**, 1, 81. (b) Feltham, K. O.; Hayter, R. G. *J. Chem. Soc.* **1964**, 4587.

complex **4**, it displays additional contacts with both oxygen atoms of the diketone and a weak bond with one nitrogen of the bipy ligand. The Tl–O distances of 2.904(4) and 2.959(4) Å are now similar to those in complex **1**, and the Tl–N bond distance (2.874(5) Å) compares well with that in $[\text{AuTl}(\text{C}_6\text{Cl}_5)_2(\text{bipy})_{0.5}]_n$ (2.839(8) Å)¹⁰ and is longer than those found in related Au/Tl complexes containing 4,4'-bipyridine as ligand (Tl–N distances ranging from 2.641(9) to 2.785(3) Å).^{7b,10}

On the other hand, the presence of a bipy ligand in **4** is probably the reason for the interesting difference observed in the crystal structures of **3** and **4**. Although, in both compounds, acetylacetonone appears in its enol mode as clearly indicated by the geometry at the central carbon atom [C(41)–C(42)–C(43) = 122.8(8) (3) and 127.6(5)° (4)], the C–O distances (1.277(8) and 1.314(9) Å in **3** and 1.324(7) and 1.238(7) Å in **4**) are not significantly different, and they are all shorter than would be expected for a C–O single bond, which suggests a high delocalization of the hydrogen atom in question. It means that the OH groups are involved in the formation of hydrogen bonds, although they are different in both cases. Thus, in complex **3** it is an intramolecular O–H···O bond (see Table 5) giving rise to a six-membered ring as shown in Figure 3, while **4** displays an intermolecular O–H···N bond (Table 5) between the OH and the free nitrogen atom of an adjacent molecule or an O···H–N bond between an oxygen of a deprotonated acacH and a N–H of a protonated bipy of an adjacent molecule of **4** resulting in the formation of dimers (see Figure 4).

Finally, each metallic center displays several metal–chlorine contacts within the range of 3.293(1)–3.406(3) Å for gold or 3.168(2)–3.647(2) Å for thallium that contribute to the stabilization of the structure.

Optical Properties. Complexes **1–4** show similar optical behavior, displaying strong bright emissions when irradiated with UV–vis radiation in the solid state at room temperature and at 77 K and, additionally, in fluid solutions. Thus, complexes **1–4** display a strong luminescence ranging from greenish yellow to orange at varying excitation energy maxima. For instance, complex **1** emits at 556 nm (excitation at 400 nm), complex **2** at 568 nm (excitation at 480 nm), complex **3** at 569 nm (excitation at 500 nm), and complex **4** at 608 nm (excitation at 475 nm) in solid state at room temperature.

Neither the gold(I) or thallium(I) precursors nor ketones or bipyridine ligands are luminescent at similar energies suggesting that the emissions are probably a result of the interaction between the metal centers. Similar assignments have been reported for systems containing the same metal atoms and oxygen or nitrogen donor ligands.^{2c,2d,6–10,20}

The luminescence of some of these complexes is temperature dependent, and thus, measurements carried out in solid state at 77 K produce a red shift of the emissions in the case of complexes **2–4** [excitation at 440 nm, emission at 600

nm (**2**); excitation at 475 nm, emission at 571 nm (**3**); and excitation at 475 nm, emission at 617 nm (**4**)], similar to the behavior found in other homo- and hetero-polynuclear gold complexes which could be related to the thermal contraction that leads to a reduction in the metal–metal distances reducing the band gap energy. Nevertheless, it is extremely interesting to note that, in the case of the previously reported complex $[\text{Au}_2\text{Tl}_2(\text{C}_6\text{Cl}_5)_4]\cdot\text{Me}_2\text{C}=\text{O}$ (**1**), the emission energy does not depend on the temperature. This phenomenon, which is described as *luminescence rigidochromism*,²¹ is not fully understood and is assigned to a substantial dependence of the emission maxima on the environmental rigidity; it has been described in other luminescent gold-heteropolynuclear systems.^{7b,22} It is important to note that the metal–metal bond distances and angles are in the same range for the four complexes, and consequently, the butterfly arrangement of the metals is not likely to be responsible for this effect.

In each case, the lifetime measurements determined by the phase-modulation technique in the solid state at room temperature display two components within the microsecond time scale: $\tau_1 = 26.0 \mu\text{s}$, $\tau_2 = 0.5 \mu\text{s}$, and $\chi^2 = 1.11$ for **2**; $\tau_1 = 1.71 \mu\text{s}$, $\tau_2 = 0.37 \mu\text{s}$, and $\chi^2 = 1.21$ for **3**; and $\tau_1 = 2.92 \mu\text{s}$, $\tau_2 = 0.5 \mu\text{s}$, and $\chi^2 = 0.98$ for **4**. These values are similar to those found for complex **1** ($\tau_1 = 2 \mu\text{s}$ and $\tau_2 = 0.7 \mu\text{s}$)^{7c} and could indicate that the emission probably originates from an excited state of triplet parentage and, consequently, is tentatively assigned as phosphorescence. Interestingly, these lifetimes are similar to that found in the gold–thallium metalcryptand reported by Catalano,^{20a} which was also assigned as a phosphorescent emission, and significantly larger than those reported in other luminescent extended gold–thallium chains that were assigned as fluorescence processes, as a consequence of transitions between gold and thallium centers, which give rise to excitons delocalized along the chains.^{2c,2d,6,7a,7b,9,10}

The luminescent behavior observed for these complexes in solution also differs from the previously reported gold–thallium chains. Thus, while those extended chains became colorless when dissolved in coordinating solvents such as acetone or tetrahydrofuran, a result that was interpreted as being caused by the rupture of the interaction between the metallic centers, these butterfly-type complexes, **2–4**, display strong luminescence in solution, revealing the solvent dependence of the emission, similar to the behavior found in complex **1**^{7c} (see Figure 5). For instance, THF, acetonitrile, or acetone solutions of **1–4** show emissions at 528 (excitation at 358 nm in THF), 539 (excitation at 346 nm in CH₃CN), or 566 nm (excitation at 356 nm in Me₂C=O) for **1**; 496 (excitation at 354 nm in THF), 506 (excitation at 350 nm in CH₃CN), or 521 nm (excitation at 346 nm in Me₂C=O) for **2**; 530 (excitation at 380 nm in THF) or 580 nm (excitation at 380 nm in Me₂C=O) for **3**; and 510 (excitation

(20) (a) Catalano, V. J.; Bennett, B. L.; Kar, H. M. *J. Am. Chem. Soc.* **1999**, *121*, 10235. (b) Burini, A.; Bravi, R.; Fackler, J. P., Jr.; Galassi, R.; Grant, T. A.; Omary, M. A.; Pietroni, B. R.; Staples, R. J. *Inorg. Chem.* **2002**, *39*, 3158.

(21) (a) Wrighton, M.; Morse, D. L. *J. Am. Chem. Soc.* **1974**, *96*, 998. (b) Itokazu, M. K.; Polo, A. S.; Murakami Iha, N. Y. *J. Photochem. Photobiol., A* **2003**, *160*, 27.
(22) Wang, S.; Garzón, G.; King, C.; Wang, J. C.; Fackler, J. P., Jr. *Inorg. Chem.* **1989**, *28*, 4623.

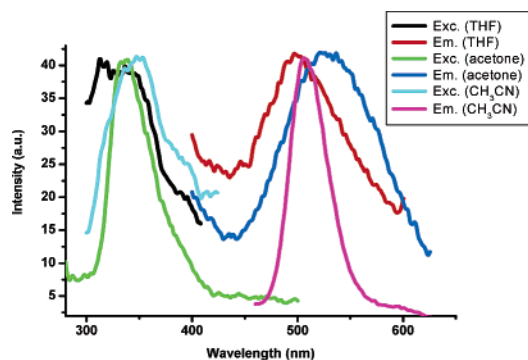


Figure 5. Luminescence spectra in solution for complex 2.

at 400 nm in THF), 575 (excitation at 380 nm in CH_3CN), or 560 nm (excitation at 350 nm in $\text{Me}_2\text{C}=\text{O}$) for **4**. In all cases the emissions are independent of the excitation wavelengths. Nevertheless, the difference between the positions of the maxima seems to be significant despite the broadness of the bands.

The absorption spectra in degassed tetrahydrofuran for these complexes display a similar pattern with strong absorption band located at 306 (**1**), 310 (**2**), 305 (**3**), and 310 nm (**4**), which are tentatively assigned to $n \rightarrow \pi^*$ transitions²³ and that are red-shifted compared to the spectra of the ketones in the same solvent, probably the result of the coordination of the ketone groups to the metal centers. In addition, the four complexes show small shoulders at 386 (**1**), 391 (**2**), 386 (**3**), and 392 nm (**4**) (see Supporting Information), values that are close to the maximum excitation energies obtained in the same solvent for complexes **3** and **4**, perhaps indicating that these absorptions give rise to the emissions. The assignment of these bands is difficult because the spectra are fairly featureless, nevertheless the absence of these bands in the absorption spectra of the precursor complexes, ketones or bipyridine seems to indicate that these absorptions arise from the metal–metal interactions remaining in solution (see below), although a ligand-to-metal charge-transfer process cannot be excluded.

In addition, the values of the emissions are close in energy to those observed in the solid state. Nevertheless, the small variation in the emission energy could be indicative of an influence of the solvent molecules with donor capabilities

on the excited states responsible for the emissions. In this context, the previously reported theoretical TD-DFT calculations for the simplified model system $[\text{Au}_2\text{Tl}_2(\text{C}_6\text{H}_5)_4]^{7c}$ suggested that the orbital from which the emission was produced was almost completely based on both thallium atoms, its origin being in the bis(perhalopheny)gold(I) units (*i.e.*, a transition that can be considered as metal-to-metal charge transfer (MMCT) in origin), although excited states arising from interactions between gold and thallium centers cannot be excluded. As these metals display weak interactions in the solid state (see crystal structures), it is likely that these contacts are also preserved to some extent in solution. Nevertheless, the participation of the ketone or bipyridine ligands cannot be excluded because the small variations of the luminescence energies in solution may be related to the presence of such solvent/ligand molecules by formation of exciplexes in the excited state. Unfortunately, none of these complexes are soluble in common noncoordinating solvents, which would allow us to confirm this possibility. Finally, these results also agree with results published recently by some of us in relation to the existence of a thallium–thallium interaction in the solid state with the presence of luminescence both in solution and in the solid state.⁹ However, by mixing TlPF_6 with any of the ketones employed in this work, nonluminescent solutions result, which seems to indicate that the gold centers are somehow necessary to give the luminescent species.

Finally, the luminescence measurements in solution at concentrations of 10^{-2} or 10^{-4} M lead to similar results for all the complexes indicating that at both concentrations similar emitting species exist.

In short, taking into account all these data, we can suggest the possible existence of species with $\text{Tl}\cdots\text{Tl}$ interactions in solution.

Acknowledgment. This work was supported by the D.G.I. (MEC)/FEDER (CTQ2004-05495).

Supporting Information Available: X-ray crystallographic files in CIF format for the structural characterization of complexes **2–4**. Experimental and simulated powder XRD patterns for complex **1**. Gold L_{III} EXAFS spectra for **1** in the solid state and in a solution of acetone and absorption spectrum in degassed THF for complex **4**. This material is available free of charge via the Internet at <http://pubs.acs.org>.

IC050060B

(23) Pretsch, E.; Bühlmann, P.; Affolter, C. *Structure Determination of Organic Compounds. Tables of Spectral Data*; Springer-Verlag: Berlin, 2000.